

- X-100, 0.5% deoxycholate, 0.1% SDS, 10% glycerol, 1 mM PMSF, 10 $\mu\text{g/ml}$ of leupeptin, and 10 $\mu\text{g/ml}$ of aprotinin. The ZPR1 immunoprecipitates were examined by protein immunoblot analysis with the monoclonal EGFR antibody 20.3.6 (18).
21. Membranes were prepared from A-431 cells and from CHO T cells that express the human insulin receptor. Briefly, the cells were serum-starved for 2 hours and washed with HEPES-buffered saline supplemented with 10 mM EDTA. The cells were lysed in 20 mM Tris (pH 7.4), 2 mM EDTA, 2 mM sodium pyrophosphate, 25 mM sodium β -glycerophosphate, 1 mM sodium orthovanadate, 25 mM NaCl, 1 mM PMSF, 10 $\mu\text{g/ml}$ of leupeptin, and 10 $\mu\text{g/ml}$ of aprotinin. Nuclei and unbroken cells were removed by centrifugation, and membranes in the supernatant fraction were recovered by centrifugation (30 min) at 100,000g. The membranes were washed with 25 mM HEPES (pH 7.4). Protein kinase assays were performed with 100 μg of membranes incubated with 5 μM [γ - ^{32}P]adenosine triphosphate (10 $\mu\text{Ci/nmol}$), 50 mM HEPES, 12 mM MgCl_2 , 2.5 mM MnCl_2 , and 100 μM sodium orthovanadate (final volume = 40 μl) at 4°C. The effect of adding 5 μg of GST or GST-ZPR1 was examined. The EGFR phosphorylation was examined in assays without and with 100 nM EGF, and the reactions were terminated after 30 s. The insulin receptor phosphorylation was examined in assays without and with 100 nM insulin, and the reactions were terminated after 2 min. The incorporation of [^{32}P]phosphate into the receptors was determined after immunoprecipitation by SDS-PAGE and Phosphor-Imager analysis.
22. A-431 cells were cultured on glass cover slips (22-mm squares; Corning). The cells were rinsed briefly with phosphate-buffered saline (PBS) and fixed at -20°C with methanol (5 min) and acetone (2 min). DNA was detected with the monoclonal antibody 1.D12 [B. L. Kozin *et al.*, *J. Immunol.* **133**, 2554 (1984)], EGFRs were detected with the monoclonal antibody 528 [T. Kawamoto *et al.*, *Proc. Natl. Acad. Sci. U.S.A.* **80**, 1337 (1983)] (American Type Culture Collection), the Golgi region was detected with a human antibody to a Golgi-associated antigen [M. J. Fritzer, K. J. Griffith, E. K. L. Chan, *Mol. Biol. Cell* **5**, 1043 (1994)], and ZPR1 was detected with a rabbit polyclonal antibody to the peptide NDMK-TEGYEAGLAPQ (17, 18). The incubation with the primary antibodies (1 hour) was done at 25°C. The cover slips were washed three times with PBS and incubated (1 hour) with species-specific secondary antibodies coupled to fluorescein or rhodamine (Caltag Laboratories). The cover slips were washed three times with PBS and mounted on slides with Vectashield media (Vector Laboratories). Control experiments with preimmune immunoglobulin and competition analysis with antigen demonstrated the specificity of the ZPR1 immunofluorescence. Laser microscopy was done with an MRC-600 confocal laser scanning microscope with an argon-krypton mixed gas laser (Bio-Rad) fitted to a Zeiss Axiovert

epifluorescence microscope with an oil immersion objective lens (1.4 numerical aperture; 63 \times). Images were collected from a single focal plane (approximately 0.4 μm) with the use of Kalman averaging of 30 scans (Bio-Rad COMOS program). The rhodamine and fluorescein images were collected simultaneously, digitized, and subsequently merged. Differential interference contrast (DIC) images were collected after fluorescence imaging. The images were recorded on Kodak Ektar 25 film.

23. We thank the following for reagents: A. Ross for the TrkA baculovirus, A. Kazlauskis for pCMV5-PDGFR β , R. L. Lewis for pCMV5-INS-R, and pCMV5-IGF1-R, M. Weber for pCMV-HA-ERK2, N. Ahn for pCMV-HA-MKK1, M. Hayman for the monoclonal antibody to the EGFR 20.3.6, K. M. Pollard for the fibrillar antibody 72B9, K. Siddle for the monoclonal antibody to the insulin receptor CT-1, A. Ross for the rabbit polyclonal antibody to TrkA 203, R. L. Rubin for monoclonal antibody 1.D12, and E. K. L. Chan for human antibody to a Golgi-associated antigen. We also thank W. Royer for assistance with computer graphics; T. Gilbert for assistance with spectroscopic analysis; and M. Roberts for secretarial assistance. Confocal microscopy was supported by the Lucille P. Markey Charitable Trust. R.J.D. is an Investigator of the Howard Hughes Medical Institute. Supported by grant R01-CA58396 from the National Cancer Institute.

4 December 1995; accepted 18 April 1996

Punctuated Evolution Caused by Selection of Rare Beneficial Mutations

Santiago F. Elena,* Vaughn S. Cooper, Richard E. Lenski

For more than two decades there has been intense debate over the hypothesis that most morphological evolution occurs during relatively brief episodes of rapid change that punctuate much longer periods of stasis. A clear and unambiguous case of punctuated evolution is presented for cell size in a population of *Escherichia coli* evolving for 3000 generations in a constant environment. The punctuation is caused by natural selection as rare, beneficial mutations sweep successively through the population. This experiment shows that the most elementary processes in population genetics can give rise to punctuated evolutionary dynamics.

The debate over punctuated equilibria (1) in evolutionary biology revolves around two distinct issues. One issue is whether, and how often, the actual dynamics of evolutionary change are punctuated by alternating periods of rapid change and relative stasis. This is an empirical issue, and the answer may depend on the coarseness of the time scale over which observations are made (2). The other issue concerns the processes responsible for any punctuation that does occur. It has been argued that punctuation involves the complex population genetic processes that are believed to play an important role in speciation (3). For example, punctuation might be precipitated by population bottlenecks that promote

random genetic drift and rapid transitions between alternative adaptive peaks (4). This view may be supported by an association between rates of anagenesis (change within a lineage) and cladogenesis (branching of lineages), but the generality and causal mechanism of this association have been disputed (1, 3, 5).

Our study builds upon earlier work (6, 7) on evolution in experimental populations of the bacterium *E. coli* B. Each population was founded from a single cell, allowed to expand to $\sim 5 \times 10^8$ cells, and then serially transferred for 1500 days (10,000 generations) in glucose-limited minimal medium (8). At each transfer, the minimum population size was $\sim 5 \times 10^6$ cells. The strain used in this experiment lacks any mechanism for genetic exchange; mutations therefore provided the sole source of genetic variation. Some 10^6 mutations occurred every day in each population (9). We did not

artificially select cells on the basis of any phenotypic property. However, any mutation that conferred some competitive advantage in exploiting the experimental environment would have been favored by natural selection. Such an advantage might involve more rapid uptake of glucose, more efficient catabolism, or any number of other physiological changes (10). We monitored two characters, mean fitness and average cell size, in the evolving populations. Fitness was measured by allowing derived and ancestral cells to compete against one another, and it is expressed as the ratio of their realized growth rates (6).

When the evolving populations were sampled at a frequency of once every 500 generations, the trajectories for both mean fitness and average cell size were well fit by a hyperbolic model (7); that is, the rate of change for each character decreased over time from an initially rapid rate, such that the character appeared to be approaching some asymptotic value. However, when mean fitness was measured every 100 generations over the period of fastest change (the first 2000 generations), a step-function model, in which periods of stasis were interrupted by episodes of rapid change, gave a better fit to the data than did the hyperbolic model (7). Evidently, it was necessary to make measurements at sufficiently high frequency to resolve the punctuated dynamics.

Step-like dynamics are predicted for mean fitness by a simple model in which successive beneficial mutations sweep through an evolving population by natural selection (5, 6, 11). Consider the initial appearance of a beneficial mutation (which

Center for Microbial Ecology, Michigan State University, East Lansing, MI 48824, USA.

*To whom correspondence should be addressed. E-mail: selena@ant.css.msu.edu

is not subsequently lost by random drift) in a large population. Many generations are required for the beneficial allele to reach a frequency at which it has an appreciable effect on mean fitness, but then relatively few generations are required for that allele to become numerically dominant (12). There may also be a substantial waiting period before a beneficial mutation even occurs, which will further lengthen the intervals of stasis between bouts of rapid change in mean fitness. Of course, mean fitness is a measure of performance and therefore cannot be measured by paleontologists. However, we also observed steplike dynamics for a conspicuous morphological character.

The evolutionary trajectory for average cell size in one population over the course of 3000 generations (Fig. 1) was fit by a step-function model (7) with the Boolean form

$$\bar{x}_t = c_0 + \sum_{i=1}^n c_i \text{ (if } t \geq T_i \text{)} \quad (1)$$

where \bar{x}_t is the average cell size at time t , c_0 is the ancestral cell size, c_i is the change in cell size during the i th step, T_i is the time at which the i th step occurs, and n is the number of discrete steps used in a given model. A model with six discrete steps gave the best fit to the data (Table 1), on the basis of the criterion that the addition of any step had to produce a significant ($P < 0.05$) reduction in the residual sum of squares. The six-step model also provides a significantly better fit than does a continuous hyperbolic model, which requires three fewer degrees of freedom [$F(3,25) = 135.32$, $P < 0.0001$].

Average cell size and mean fitness during the first 2000 generations [the fitness data are from (7)] were highly correlated ($r = 0.954$, $n = 21$, $P < 0.0001$) (Fig. 2), but we do not know whether cell size affects fitness directly or whether they are correlated with some other characters that are the actual targets of selection (13). For example, larger cells might have a direct selective advantage if they can mobilize their extra biomass to commence growth sooner than smaller cells when the population is transferred each day into fresh medium (14). Alternatively, faster growing *E. coli* cells tend to be larger phenotypically than slower growing cells (15), and so an increase in average cell size might simply be a correlated response to selection for faster growth (14).

We are also interested in examining the correspondence between the step models that were separately fit to the data for mean fitness [analysis in (7)] and average cell size

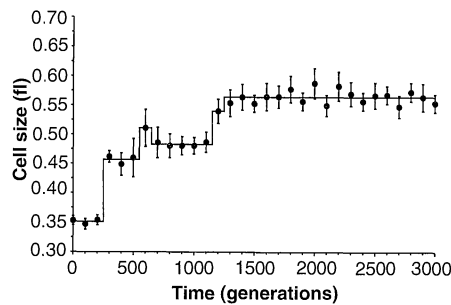


Fig. 1. Change in average cell size (1 fl = 10^{-15} L) in a population of *E. coli* during 3000 generations of experimental evolution. Each point is the mean of 10 replicate assays (22). Error bars indicate 95% confidence intervals. The solid line shows the best fit of a step-function model to these data (Table 1).

(Fig. 1). The former analysis yielded four significant steps, with the following samples grouped together: generations 0 to 200, 300 to 500, 600 to 1200, and 1300 to 2000. The latter analysis yielded six significant steps, with samples grouped as follows: generations 0 to 200, 300 to 500, 600, 700 to 1100, 1200, and 1300 to 3000. Thus, there are only two discrepancies among the 21 samples for which both cell size and fitness were measured. In both cases, the cell size data suggest extra steps that were not supported by the fitness data. One explanation to account for these discrepancies is that there is an actual discordance between the episodes of rapid change in cell size and fitness. Hypothetically, a mutation affecting cell size might have drifted to fixation, for example, between generations 600 and 700. This explanation seems unlikely, given the large population size and short time interval involved. The more trivial explanation is that these discrepancies reflect statistical uncertainties rather than any real biological discordance. One possibility is that a difference resulting from sampling error was erroneously accepted as real. Both of the steps in question were supported only rather marginally by the cell size data (Table 1, P values of 0.023 and 0.021). Another possibility is that the fitness data lacked

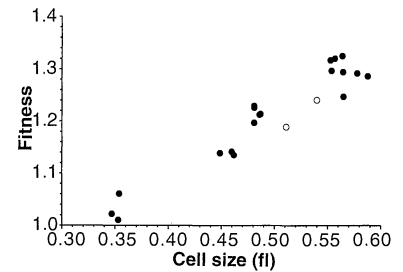


Fig. 2. Correlation between average cell size and mean fitness, each measured at 100-generation intervals for 2000 generations. Fitness is expressed relative to the ancestral genotype and was obtained from competition experiments between derived and ancestral cells (6, 7). The open symbols indicate the only two samples assigned to different steps by the cell size and fitness data.

sufficient power to resolve certain real differences. Consistent with this scenario, the generation-600 sample gave the lowest estimate of mean fitness of the seven samples assigned to the corresponding step, whereas the generation-1200 sample gave the highest estimate (7).

In short, the correspondence between the dynamics for cell size and fitness is quite strong. The only two discrepancies in the step models appear to be minor and are probably the result of statistical ambiguities. Therefore, the evidence taken as a whole supports the inference that the observed changes in average cell size are temporally associated with the successive sweeps of beneficial mutations. This temporal association may arise by either of two population genetic mechanisms. The first hypothesis is that changes in cell size are either directly selected or are pleiotropic side effects of the mutations that confer the selective advantage. The second hypothesis is that mutations affecting cell size have hitchhiked to high frequency along with the mutations that actually confer the selective advantage. We favor the former hypothesis because all 12 replicate populations steadily increased in cell size (7). Such an outcome is very unlikely under the hitchhiking hypothesis, unless there are many more muta-

Table 1. Analysis of variance comparing the fit of models with different numbers of steps to the trajectory for average cell size shown in Fig. 1. A partial- F test (23) was used to assess the significance of adding an additional step to the model. Each step uses one degree of freedom. Groupings indicate the assignment of the samples taken at 100-generation intervals to successive steps in the model (24). SSR, residual sum of squares; d.f., residual degrees of freedom; and P , significance level.

Model	Groupings (100 generations)	SSR	d.f.	Partial F	P
1 step	0-30	0.1420	30	—	—
2 steps	0-11, 12-30	0.0413	29	70.83	<0.0001
3 steps	0-2, 3-11, 12-30	0.0054	28	185.32	<0.0001
4 steps	0-2, 3-5, 6-11, 12-30	0.0035	27	14.61	0.0007
5 steps	0-2, 3-5, 6, 7-11, 12-30	0.0029	26	5.83	0.023
6 steps	0-2, 3-5, 6, 7-11, 12, 13-30	0.0023	25	6.07	0.021
7 steps	0-2, 3-5, 6, 7-11, 12, 13-17, 18-30	0.0022	24	1.30	0.266

tions that cause cell size to increase than those that cause it to decrease.

These questions notwithstanding, our data clearly demonstrate a pattern of punctuated evolution for a quantitative morphological character. Moreover, this pattern arose in a simple experimental system without any population subdivision (which promotes cladogenesis), and the punctuated changes were largely (if not entirely) caused by the successive fixation of several beneficial mutations. Millions of mutations occurred during these thousands of generations (9), but evidently beneficial mutations of large effect were quite rare (16). The experimental population was strictly asexual, which may have increased our ability to resolve punctuated changes. However, any difference between sexual and asexual populations with respect to the dynamics of adaptive evolution (17) breaks down when two conditions are met: (i) standing genetic variation for fitness is exhausted, as will eventually happen in any constant environment (18), and (ii) beneficial mutations are so rare that they occur as isolated events (11, 17). To the extent that these conditions are fulfilled in nature, then the selective sweep of beneficial alleles through a population might explain some cases of punctuated evolution in the fossil record. In any case, our experiment shows that punctuated evolution can occur in bacterial populations as a consequence of the two most elementary population genetic processes: mutation and natural selection.

REFERENCES AND NOTES

1. N. Eldredge and S. J. Gould, in *Models in Paleobiology*, T. J. M. Schopf, Ed. (Freeman, San Francisco, 1972), pp. 82-115; P. G. Williamson, *Nature* **293**, 437 (1981); B. Charlesworth, R. Lande, M. Slatkin, *Evolution* **36**, 474 (1982); P. D. Gingerich, *Syst. Zool.* **33**, 335 (1984); J. Levinton, *Genetics, Paleontology and Macroevolution* (Cambridge Univ. Press, New York, 1988); S. J. Gould and N. Eldredge, *Nature* **366**, 223 (1993).
2. F. L. Bookstein, P. D. Gingerich, A. G. Kluge, *Paleobiology* **4**, 120 (1978); L. R. Ginzburg, *ibid.* **7**, 426 (1981); P. D. Gingerich, *Science* **222**, 159 (1983).
3. S. J. Gould, in *Perspectives on Evolution*, R. Milkman, Ed. (Sinauer, Sunderland, MA, 1982), pp. 83-104.
4. C. M. Newman, J. E. Cohen, C. Kipnis, *Nature* **315**, 400 (1985).
5. J. R. G. Turner, in *Patterns and Processes in the History of Life*, D. M. Raup and D. Jablonski, Eds. (Springer, Berlin, 1986), pp. 183-207.
6. R. E. Lenski, M. R. Rose, S. C. Simpson, S. C. Tadler, *Am. Nat.* **138**, 1315 (1991).
7. R. E. Lenski and M. Travisano, *Proc. Natl. Acad. Sci. U.S.A.* **91**, 6808 (1994).
8. Bacteria were grown at 37°C in 10 ml of Davis minimal medium supplemented with glucose at 25 µg ml⁻¹ (6). Each day, the stationary-phase population was diluted 100-fold into fresh medium, which allowed ~6.6 (= log₂ 100) generations of binary fission per day.
9. The total mutation rate equals the product of the number of cell replications per day (~5 × 10⁹) and the genomic mutation rate [which is ~0.0025 for *E. coli* (19)].

10. M. Travisano and R. E. Lenski, *Genetics* **143**, 15 (1996).
11. P. A. Johnson, R. E. Lenski, F. C. Hoppensteadt, *Proc. R. Soc. London Ser. B* **259**, 125 (1995).
12. Let $R(0)$ be the initial ratio of the population of a mutant genotype to that of its progenitor and let $R(t)$ be that ratio at time t . Then $\ln R(t) = \ln R(0) + st$, where s is the selection rate constant (20). For example, if $s = 0.46$ per day, which corresponds to a relative fitness of 1.1 (= 1 + $s/\ln 100$) in our experiment (6), then it takes 30 days (200 generations) for a single mutant to increase to a frequency of 10% in a population of 10⁷, but only 5 more days are needed to reach 50%.
13. S. J. Arnold, *Am. Zool.* **23**, 347 (1983).
14. F. Vasi, M. Travisano, R. E. Lenski, *Am. Nat.* **144**, 432 (1994).
15. F. C. Neidhardt, J. L. Ingraham, M. Schaechter, *Physiology of the Bacterial Cell* (Sinauer, Sunderland, MA, 1990).
16. Beneficial mutations of small effect would require many more generations to go to fixation than would those detected in this experiment. For example, a mutation having a fitness advantage of only 0.1% would require 3000 days (20,000 generations) to reach a frequency of 10% (12). Such a mutation would also be 100 times more likely to be lost by genetic drift than would one with a 10% advantage (21), and the former would be competitively excluded by the latter if they occurred together as different lineages in an asexual population (6, 17).
17. H. J. Muller, *Am. Nat.* **66**, 118 (1932).
18. D. S. Falconer, *Introduction to Quantitative Genetics* (Longman, London, ed. 2, 1981).
19. J. W. Drake, *Proc. Natl. Acad. Sci. U.S.A.* **88**, 7160 (1991).
20. D. E. Dykhuizen and D. L. Hartl, *Microbiol. Rev.* **47**, 150 (1983).
21. J. B. S. Haldane, *Proc. Cambridge Philos. Soc.* **23**, 838 (1927).
22. We measured average cell size using a Coulter particle counter (model ZM and channelyzer model 256), which measures the volume displaced by each of several thousand cells as they pass through a small aperture. Cells were grown to stationary-phase density in the same medium used in the evolution experiment (6, 8, 14). Replicate assays were run in complete blocks to avoid possible confounding effects of temporal variation in experimental conditions.
23. D. G. Kleinbaum and L. L. Kupper, *Applied Regression Analysis and Other Multivariable Methods* (Duxbury, North Scituate, MA, 1978).
24. The Levenberg-Marquard numerical method used to fit the models to the data requires an initial value for each parameter; several sets of initial values were tested for convergence.
25. We thank J. A. Mongold for help with the experiments; A. F. Bennett, J. E. Cohen, D. J. Hall, J. A. Mongold, and P. D. Sniegowski for discussion and comments; and A. G. Clark for suggesting that we obtain these data. This work was supported by a fellowship from the Spanish Ministerio de Educación y Ciencia to S.F.E., a fellowship from Michigan State University to V.S.C., and a grant from NSF (DEB-9421237) to R.E.L.

22 January 1996; accepted 29 April 1996

Aberrant B Cell Development and Immune Response in Mice with a Compromised BCR Complex

Raul M. Torres,*† Heinrich Flaswinkel, Michael Reth, Klaus Rajewsky

The immunoglobulin α (Ig- α)-Ig- β heterodimer is the signaling component of the antigen receptor complex on B cells (BCR) and B cell progenitors (pre-BCR). A mouse mutant that lacks most of the Ig- α cytoplasmic tail exhibits only a small impairment in early B cell development but a severe block in the generation of the peripheral B cell pool, revealing a checkpoint in B cell maturation that ensures the expression of a functional BCR on mature B cells. B cells that do develop demonstrate a differential dependence on Ig- α signaling in antibody responses such that a signaling-competent Ig- α appears to be critical for the response to T-independent, but not T-dependent, antigens.

Surface expression of, and signaling by, Ig on B lymphocytes is dependent on both Ig- α and Ig- β (1-5). The signaling capacity of these two molecules, which are expressed as heterodimers in the pre-BCR and BCR (2-5), has been attributed to the presence of an immunoreceptor tyrosine-based activation motif (ITAM) within both intracellular domains (6). Indeed, BCR signaling is severely compromised when the Ig- α ITAM

is mutated or deleted in a myeloma cell line (3). In the presence of wild-type Ig- β , the extracellular and transmembrane domains of Ig- α are sufficient for surface Ig expression (3). Thus, by truncation of the Ig- α cytoplasmic tail, a mouse mutant can be generated that retains B cell surface Ig expression (Fig. 1) but is compromised in Ig- α signaling (3, 7), allowing the identification of a point or points at which a pre-BCR or BCR signal is critical for B cell development or function (or both).

Homologous recombination in embryonic stem (ES) cells (8) resulted in an ES cell line (E Δ 6) in which a stop codon was introduced in exon four of *mb-1* (Fig. 1A). The mutated locus (*mb-1* ^{Δ c/ Δ c}) encodes a truncated Ig- α molecule whose cytoplasmic tail

R. M. Torres and K. Rajewsky, Institute for Genetics, University of Cologne, Weyertal 121, D-50931 Cologne, Germany.

H. Flaswinkel and M. Reth, Max Planck Institute for Immunobiology, 79108 Freiburg, Germany.

*To whom correspondence should be addressed.

†Present address: Basel Institute for Immunology, Grenzacherstrasse 487, Postfach CH-4005 Basel, Switzerland.